

# STOCHASTIC INTEREST RATE MODEL: BOND OPTION AND SWAPTIONS

XIAOLU XIONG, LUJIA YANG, AND ZIYI WANG

**ABSTRACT.** The term structure of interest rates has played an essential role in pricing multiple financial derivatives. This project showed the deterministic function that can calculate bond prices assuming a two-factor Interest rate model. Empirical evidence of the analytical functions' well performance is presented compared to the Monte Carlo simulation.

The report also investigated the impact of the interest rate model parameters on the yield curve shape. The result showed us that increasing the mean reversion speed parameters increase the curvature of the yield curve and drive a higher Bond Yield. Increasing the mean reversion level can reduce the steepness of the bond yield curve. Increasing the volatility parameters brings higher bond prices with more interest rate risk.

In addition, this report also presented the analytical expression of a specific bond option. The analytical result is also backed by comparing two different Monte Carlo simulations. Lastly, we researched the implied volatility of a swaption. The implied volatility shows a volatility skew/ smile with more wights on the left side, which indicates that in the money swaption is more valuable than out of the money swaption. The "smile" shape become more obvious as maturity (T1) decrease. Investors can select appropriate investment products to hedge the interest rate risk based on their risk appetite and monetary needs.

## CONTENTS

<b>1. Introduction</b>	<b>2</b>
1.1. Motivation	2
1.2. Background	2
1.3. Project Structure and Goal	2
<b>2. Methodology</b>	<b>3</b>
2.1. Two Factor Vasicek Interest Rate Model	3
2.2. Bond Price Process	4
2.3. Bond Option	7
2.4. Interest Rate Swap Rate	10
2.5. Interest Rate Swaption Price	10
2.6. Implied volatility	11
<b>3. Results</b>	<b>12</b>
3.1. Base Case Assumptions	12
3.2. Bond Yield under Different Scenarios	13
3.3. Bond Option	21
3.4. Swaption Implied Volatility	24
<b>4. Conclusion</b>	<b>28</b>

## 1. Introduction

### 1.1. Motivation.

The term structure of the interest rates is one of the most important concepts in pricing fixed income securities, and interest rate derivatives such as bond options, interest rate swap and swaption as the pay-offs of these financial instruments are closely correlated to the interest rates. It's practically important to understand the relationship between an interest rate model and the financial derivatives pricing process. Nowadays, the economies around the world are becoming more integrated. Due to the economic impacts stemming from COVID-19, governments lowered interest rates to support economic activity. It's worth focusing on the two-factor interest rate model to understand the impact of short-term and long-term interest rates on the derivatives' prices.

### 1.2. Background.

To rationale the theories introduced in this report, it's necessary to introduce a few concepts. A zero-coupon bond with maturity date  $T$  and face value 1 has a fixed payoff at maturity. The term structure of the interest rates and the maturity can determine the bond's yield. Under a no-arbitrage condition, there exists a risk-neutral measure under which the price of the  $T$ -maturity zero coupon bond can be estimated as an expected value of an integral of interest rate under the risk-neutral measure. Intuitively, the price of this bond can be simulated if the distribution of the short rate under a risk-neutral measure is given. The predicted bond price can then be used to predict a swaption's pricing process.

### 1.3. Project Structure and Goal.

In this project, we will calibrate a two-factor Vasicek model to describe the  $T$ -maturity bond price process. Assuming the given Vasicek model for interest rate, the price of the  $T$ -maturity zero-coupon bond can be expressed as an analytical formula. We will show the process of solving the PDE that is satisfied by the zero-coupon bond to derive the formula. Then to evaluate the correctness of the formula derived using the PDE approach, the Monte-Carlo method will be used to estimate bond yields and compare it with the analytical formulas with the same set of base parameters.

The two-factor Vasicek model can model the interest rate as Ornstein-Uhlenbeck processes, implying that the short rate process is mean-reverting with mean reversion rate and level by certain parameters. This report will also mention the effect of parameters in the model on bond yields.

The investigation of the bond pricing process can also extend to bond option pricing and swaption pricing. This project will also show the process of deriving the analytical formula for a special case of a bond option, where the underlying asset is a  $T_1$  maturity bond. The analytical formula of this bond is successfully verified by Monte Carlo simulation under both the risk-neutral and forward-neutral measures. In the end, the report will further address the relationship between the black implied volatility and strike price.

## 2. Methodology

### 2.1. Two Factor Vasicek Interest Rate Model.

In the two factor Vasicek Interest Rate Model, the long and short rate of interest  $r = (r_t)_{t \geq 0}$  is modeled as two Ornstein-Uhlenbeck processes:

$$\begin{aligned} dr_t &= \alpha(\theta_t - r_t)dt + \sigma dW_t^1 \\ d\theta_t &= \beta(\phi - \theta_t)dt + \eta dW_t^2 \end{aligned}$$

where  $W^{1,2} = (W_t^{1,2})_{t \geq 0}$  are independent risk-neutral Brownian motions, and  $\theta = (\theta_t)_{t \geq 0}$  represent the long-run rate of interest.

The above process can be modeled as per below pseudocode:

---

**Algorithm 1** Algorithm for Simulating Interest Rate Path

---

**Require:**  $i \geq 0, j \geq 0, dt \geq 0$

$r = r_0$

$\theta = \theta_0$

$j \leftarrow j + 1$

**while**  $j \leq \text{nSim}$  **do**

▷ nSim: the number of simulations

$i \leftarrow i + 1$

**while**  $i \leq \text{ndt}$  **do**

▷ ndt: the number of time steps/intervals

$dr\_t = \beta \times (\phi - \theta) \times dt + \eta \times \sqrt{dt} \times Z;$

▷ Z: a random sample from the standard normal distribution

$\theta \leftarrow \theta + dr\_t;$

$dr = \alpha \times (\theta - r) \times dt + \sigma \times \sqrt{dt} \times Z;$

$r \leftarrow r + dr;$

**end while**

**end while**

---

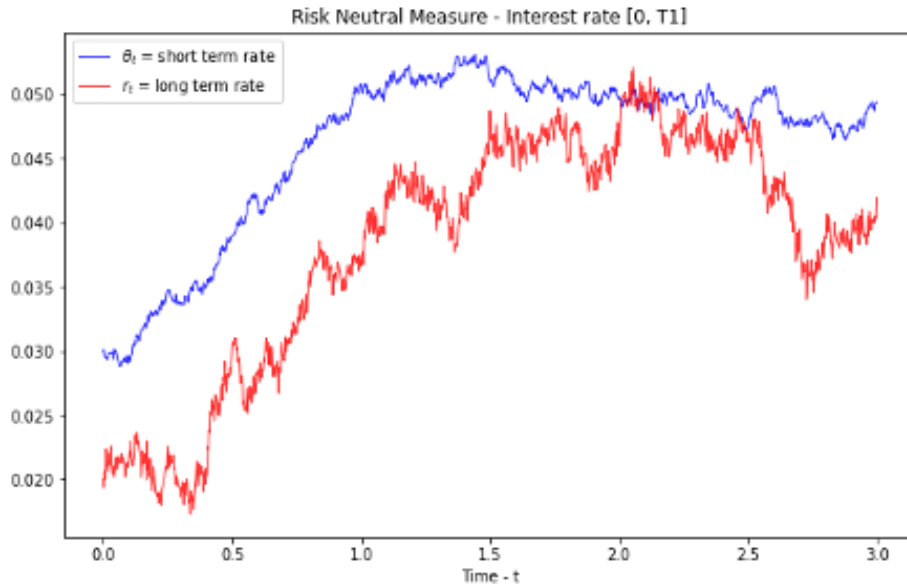


FIGURE 1. Simulated Long and Short-term Interest Rate

## 2.2. Bond Price Process.

Let the T-maturity bond price process be denoted  $P(T) = (P_t(T))_{t \in [0, T]}$ , the bond price process can be expressed as a deterministic function

$$P_t(T) = \exp(A_t(T) - B_t(T)r_t - C_t(T)\theta_t)$$

$A_t(T)$ ,  $B_t(T)$  and  $C_t(T)$  can be derived by solving the below PDE. As the T-maturity bond is an interest rate derivative of the short rate of interest. The bond pricing process should satisfies the PDE given above and the corresponding payoff function.

$$\mathbb{E}_t^{\mathbb{Q}}[e^{-\int_t^T r_s ds}] = f(t, r_t, \theta_t)$$

As the interest rate path is a two factor interest rate Vasicek Model, we have  $P_t(T) = f(t, r_t, \theta_t)$  that should satisfies:

$$\Rightarrow \begin{cases} (\partial_t + L)f = rf \\ f(T, r, \theta) = 1 \end{cases}$$

where

$$L = \alpha(\theta - r)\partial_r + \frac{1}{2}\sigma^2\partial_{rr} + \beta(\phi - \theta)\partial_\theta + \frac{1}{2}\eta^2\partial_{\theta\theta}$$

that is

$$\begin{cases} \frac{\partial f}{\partial t} + \alpha(\theta - r)\frac{\partial f}{\partial r} + \frac{1}{2}\sigma^2\frac{\partial^2 f}{\partial r^2} + \beta(\phi - \theta)\frac{\partial f}{\partial \theta} + \frac{1}{2}\eta^2\frac{\partial^2 f}{\partial \theta^2} = rf \\ f(T, r, \theta) = 1 \end{cases}$$

$$\left. \begin{aligned} \frac{\partial f}{\partial t} &= (\dot{A} - \dot{B}r - \dot{C}\theta)f \\ \frac{\partial f}{\partial r} &= -Bf \\ \frac{\partial f}{\partial \theta} &= -Cf \\ \frac{\partial^2 f}{\partial r^2} &= B^2f \\ \frac{\partial^2 f}{\partial \theta^2} &= C^2f \end{aligned} \right\} \begin{aligned} \dot{C} &= \frac{d}{dt}C_t \\ \dot{B} &= \frac{d}{dt}B_t \\ \dot{A} &= \frac{d}{dt}A_t \end{aligned}$$

$$(\dot{A} - \dot{B} - \dot{C}\theta)f + \alpha(\theta - r)(-Bf) + \frac{1}{2}\sigma^2 B^2 f + \beta(\phi - \theta)(-Cf) + \frac{1}{2}\eta^2 C^2 f = rf$$

Organize the term as follows

$$\dot{A}f - \dot{B}rf - \dot{C}\theta f + \alpha Brf - \alpha B\theta f + \frac{1}{2}\sigma^2 B^2 f - \beta\phi Cf + \beta C\theta f + \frac{1}{2}\eta^2 C^2 f = rf$$

$$\underbrace{(-\dot{C} - \alpha B + \beta C)\theta f}_{\textcircled{1}} + \underbrace{(-\dot{B} + \alpha B - 1)rf}_{\textcircled{2}} + \underbrace{(\dot{A} + \frac{1}{2}\sigma^2 B^2 - \beta\phi C + \frac{1}{2}\eta^2 C^2)f}_{\textcircled{3}} = 0$$

The above equation holds for all  $\eta$  and can be rewrite to the below corresponding ODE:

$$\begin{cases} -\dot{C} - \alpha B + \beta C = 0 \Rightarrow \dot{C} = \beta C - \alpha B & \textcircled{1} \\ -\dot{B} + \alpha B - 1 = 0 & \textcircled{2} \\ \dot{A} + \frac{1}{2}\sigma^2 B^2 - \beta\phi C + \frac{1}{2}\eta^2 C^2 = 0 & \textcircled{3} \end{cases}$$

By ②, we have that

$$\begin{aligned}
& -\dot{B} + \alpha B - 1 = 0 \\
\Rightarrow & \frac{\dot{B}}{1 - \alpha B} = -1 \\
\Rightarrow & -\frac{1}{\alpha} \frac{d}{dt} \log(1 - \alpha B) = -1 \\
\Rightarrow & \frac{d}{dt} \log(1 - \alpha B) = \alpha \\
\Rightarrow & d \log(1 - \alpha B) = \alpha dt \\
\Rightarrow & \int_t^T \log(1 - \alpha B_s) ds = \alpha(T - t) \\
\Rightarrow & \log\left(\frac{1 - \alpha B_T}{1 - \alpha B_t}\right) = \alpha(T - t) \\
\Rightarrow & \log\left(\frac{1}{1 - \alpha B_t}\right) = \alpha(T - t) \quad (B_T = 0) \\
\Rightarrow & -\log(1 - \alpha B_t) = \alpha(T - t) \\
\Rightarrow & B_t = \frac{1 - e^{-\alpha(T-t)}}{\alpha}
\end{aligned}$$

Then, by ①, we have that

$$\begin{aligned}
\frac{d}{dt}(e^{\beta(T-t)}C) &= -\beta e^{\beta(T-t)}C + e^{\beta(T-t)}\dot{C} \\
&= -\beta e^{\beta(T-t)}C + e^{\beta(T-t)}\beta C - \alpha B \\
&= -\alpha B e^{\beta(T-t)}
\end{aligned}$$

Plugging in  $B_t = \frac{1 - e^{-\alpha(T-t)}}{\alpha}$ , we have that

$$\begin{aligned}
\frac{d}{dt}(e^{\beta(T-t)}C) &= -\alpha \frac{1 - e^{-\alpha(T-t)}}{\alpha} e^{\beta(T-t)} \\
&= e^{\beta(T-t)}(e^{-\alpha(T-t)} - 1) \\
&= e^{(\beta-\alpha)(T-t)} - e^{\beta(T-t)}
\end{aligned}$$

Then, we take the integral.

$$\begin{aligned}
& (e^{\beta(T-t)}C_s)|_t^T = \int_t^T e^{(\beta-\alpha)(T-s)} ds - \int_t^T e^{\beta(T-s)} ds \\
\Rightarrow & C_T - e^{\beta(T-t)}C_t = \frac{1}{\alpha - \beta} e^{(\beta-\alpha)(T-s)}|_t^T + \frac{1}{\beta} e^{\beta(T-s)}|_t^T \\
\Rightarrow & -e^{\beta(T-t)}C_t = \frac{1}{\alpha - \beta} (1 - e^{(\beta-\alpha)(T-t)}) + \frac{1}{\beta} (1 - e^{\beta(T-t)}) \quad (C_T = 0) \\
\Rightarrow & C_t = \frac{1}{\alpha - \beta} (e^{-\alpha(T-t)} - e^{-\beta(T-t)}) + \frac{1}{\beta} (1 - e^{-\beta(T-t)})
\end{aligned}$$

Then, we simplify  $C_t$ .

$$\begin{aligned}
C_t &= \frac{1}{\alpha - \beta}(e^{-\alpha(T-t)} - e^{-\beta(T-t)}) + \frac{1}{\beta}(1 - e^{-\beta(T-t)}) \\
&= \frac{1}{\beta} + \frac{1}{\alpha - \beta}e^{-\alpha(T-t)} - \frac{1}{\alpha - \beta}e^{-\beta(T-t)} - \frac{1}{\beta}e^{-\beta(T-t)} \\
&= \frac{\alpha - \beta}{\beta(\alpha - \beta)} + \frac{\beta}{\beta(\alpha - \beta)}e^{-\alpha(T-t)} - \frac{\alpha}{\beta(\alpha - \beta)}e^{-\beta(T-t)} \\
&= -\frac{\beta}{\beta(\alpha - \beta)} + \frac{\beta}{\beta(\alpha - \beta)}e^{-\alpha(T-t)} + \frac{\alpha}{\beta(\alpha - \beta)} - \frac{\alpha}{\beta(\alpha - \beta)}e^{-\beta(T-t)} \\
&= \frac{\beta}{\beta(\alpha - \beta)}(-1 + e^{-\alpha(T-t)}) + \frac{\alpha}{\beta(\alpha - \beta)}(1 - e^{-\beta(T-t)}) \\
&= \frac{\alpha}{\alpha - \beta} \frac{-1 + e^{-\alpha(T-t)}}{\alpha} + \frac{\alpha}{\alpha - \beta} \frac{1 - e^{-\beta(T-t)}}{\beta} \\
\Rightarrow C_t &= \frac{\alpha}{\alpha - \beta} \left( \frac{1 - e^{-\beta(T-t)}}{\beta} - \frac{1 - e^{-\alpha(T-t)}}{\alpha} \right)
\end{aligned}$$

Finally, by ③, we have that

$$\begin{aligned}
&\dot{A} + \frac{1}{2}\sigma^2 B^2 - \beta\phi C + \frac{1}{2}\eta^2 C^2 = 0 \\
\Rightarrow \quad &\dot{A} = -\frac{1}{2}\sigma^2 B^2 + \beta\phi C - \frac{1}{2}\eta^2 C^2 \\
\Rightarrow \quad &A_T - A_t = \int_t^T -\frac{1}{2}\sigma^2 B_s^2 + \beta\phi C_s - \frac{1}{2}\eta^2 C_s^2 ds \\
\Rightarrow \quad &-A_t = -\frac{1}{2}\sigma^2 \int_t^T B_s^2 ds + \beta\phi \int_t^T C_s ds - \frac{1}{2}\eta^2 \int_t^T C_s^2 ds \quad (A_T = 0) \\
\Rightarrow \quad &A_t = \frac{1}{2}\sigma^2 D - \beta\phi E + \frac{1}{2}\eta^2 F
\end{aligned}$$

Further derive, we have that

$$\begin{aligned}
D &= \int_t^T B_s^2 ds = \frac{1}{\alpha^2}[(T-t) + \frac{1}{\alpha}(-\frac{3}{2} + 2e^{-\alpha(T-t)} - e^{-2\alpha(T-t)})] \\
E &= \int_t^T C_s ds = \frac{T-t}{\beta} + \frac{\alpha}{\alpha - \beta} \left( \frac{1 - e^{-\alpha(T-t)}}{\alpha^2} - \frac{1 - e^{-\beta(T-t)}}{\beta^2} \right) \\
F &= \int_t^T C_s^2 ds = \frac{T-t}{\beta^2} + \frac{1 - e^{-2\alpha(T-t)}}{2\alpha(\alpha - \beta)^2} + \frac{2(1 - e^{-\alpha(T-t)})}{\alpha\beta(\alpha - \beta)} - \frac{2\alpha(1 - e^{-(\alpha+\beta)(T-t)})}{(\alpha - \beta)^2\beta(\alpha + \beta)} \\
&\quad - \frac{2\alpha(1 - e^{-\beta(T-t)})}{(\alpha - \beta)\beta^3} + \frac{\alpha^2(1 - e^{-2\beta(T-t)})}{2(\alpha - \beta)^2\beta^2}
\end{aligned}$$

Therefore, we can conclude that the bond price process is

$$P_t(T) = \exp(A_t(T) - B_t(T)r_t - C_t(T)\theta_t)$$

where

$$\left\{ \begin{array}{l} A_t(T) = \frac{1}{2}\sigma^2 D - \beta\phi E + \frac{1}{2}\eta^2 F \\ D = \frac{1}{\alpha^2}[(T-t) + \frac{1}{\alpha}(-\frac{3}{2} + 2e^{-\alpha(T-t)} - e^{-2\alpha(T-t)})] \\ E = \frac{T-t}{\beta} + \frac{\alpha}{\alpha-\beta}(\frac{1-e^{-\alpha(T-t)}}{\alpha^2} - \frac{1-e^{-\beta(T-t)}}{\beta^2}) \\ F = \frac{T-t}{\beta^2} + \frac{1-e^{-2\alpha(T-t)}}{2\alpha(\alpha-\beta)^2} + \frac{2(1-e^{-\alpha(T-t)})}{\alpha\beta(\alpha-\beta)} - \frac{2\alpha(1-e^{-(\alpha+\beta)(T-t)})}{(\alpha-\beta)^2\beta(\alpha+\beta)} - \frac{2\alpha(1-e^{-\beta(T-t)})}{(\alpha-\beta)\beta^3} + \frac{\alpha^2(1-e^{-2\beta(T-t)})}{2(\alpha-\beta)^2\beta^2} \\ B_t(T) = \frac{1-e^{-\alpha(T-t)}}{\alpha} \\ C_t(T) = \frac{\alpha}{\alpha-\beta}(\frac{1-e^{-\beta(T-t)}}{\beta} - \frac{1-e^{-\alpha(T-t)}}{\alpha}) \end{array} \right.$$

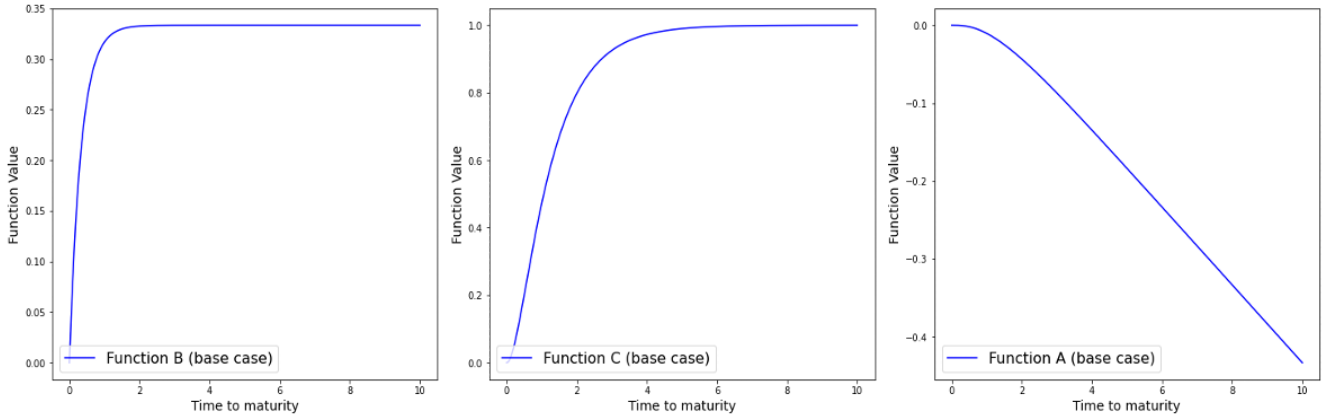


FIGURE 2. Function A, B, and C with respect to Maturity

We can observe the function behavior with respect to the time to maturity in the above figure, where the function B and C behave like a bond yield curve, with Function B steeper than Function C. Function A is a decreasing line when the time to maturity increase. Intuitively, we might expect the yield curve  $\frac{-\ln(P_t(T))}{T-t}$  have an increasing trend with decreasing growth rate as the maturity increase.

### 2.3. Bond Option.

We have a bond option paying  $(P_{T_1}(T_2) - K)_+$  at  $T_1$  where  $K = P_0(T_2)/P_0(T_1)$ . The price of this option is

$$v_t = \mathbb{E}_t^{\mathbb{Q}}[e^{-\int_t^{T_1} r_s ds} (P_{T_1}(T_2) - K)_+]$$

We use a bond of maturity  $T_1$  as a numeraire asset. Then, we have that

$$\begin{aligned}
\frac{v_t}{P_t(T_1)} &= \mathbb{E}_t^{\mathbb{Q}^{T_1}} \left[ \frac{(P_{T_1}(T_2) - K)_+}{P_{T_1}(T_1)} \right] \\
\Rightarrow \frac{v_t}{P_t(T_1)} &= \mathbb{E}_t^{\mathbb{Q}^{T_1}} \left[ \left( \frac{P_{T_1}(T_2)}{P_{T_1}(T_1)} - \frac{K}{P_{T_1}(T_1)} \right)_+ \right] \\
\Rightarrow \frac{v_t}{P_t(T_1)} &= \mathbb{E}_t^{\mathbb{Q}^{T_1}} \left[ \left( \frac{P_{T_1}(T_2)}{P_{T_1}(T_1)} - K \right)_+ \right] \quad (P_{T_1}(T_1) = 1) \\
\Rightarrow v_t &= P_t(T_1) \mathbb{E}_t^{\mathbb{Q}^{T_1}} \left[ \left( \frac{P_{T_1}(T_2)}{P_{T_1}(T_1)} - K \right)_+ \right]
\end{aligned}$$

Under  $\mathbb{Q}^{T_1}$ , we know that the interest rates satisfy the following SDE.

$$\begin{aligned}
dr_t &= (\alpha(\theta_t - r_t) - \sigma^2 B_t(T_1))dt + \sigma dW^{\mathbb{Q}^{T_1,1}} \\
d\theta_t &= (\beta(\phi - \theta_t) - \eta^2 C_t(T_1))dt + \eta dW^{\mathbb{Q}^{T_1,2}}
\end{aligned}$$

where  $W^{\mathbb{Q}^{T_1,1}}$  and  $W^{\mathbb{Q}^{T_1,2}}$  are independent Brownian motions under  $\mathbb{Q}^{T_1}$ .

Let  $X_t = \frac{P_t(T_2)}{P_t(T_1)}$  which is a  $\mathbb{Q}^{T_1}$  martingale. We have that

$$v_t = P_t(T_1) \mathbb{E}_t^{\mathbb{Q}^{T_1}} [(X_{T_1}(T_2) - K)_+]$$

Since  $P_t(T) = \exp(A_t(T) - B_t(T)r_t - C_t(T)\theta_t)$ , we can calculate  $X_t$ .

$$X_t = \frac{P_t(T_2)}{P_t(T_1)} = \exp((A_t(T_2) - A_t(T_1)) - (B_t(T_2) - B_t(T_1))r_t - (C_t(T_2) - C_t(T_1))\theta_t) = f(t, r_t, \theta_t)$$

Then, we calculate  $dX_t$ .

$$\begin{aligned}
dX_t &= 0dt + \sigma \partial_{r_t} f(t, r_t, \theta_t) dW^{\mathbb{Q}^{T_1,1}} + \eta \partial_{\theta_t} f(t, r_t, \theta_t) dW^{\mathbb{Q}^{T_1,2}} \quad (X_t \text{ is a martingale}) \\
&= -\sigma(B_t(T_2) - B_t(T_1))f(t, r_t, \theta_t) dW^{\mathbb{Q}^{T_1,1}} - \eta(C_t(T_2) - C_t(T_1))f(t, r_t, \theta_t) dW^{\mathbb{Q}^{T_1,2}} \\
&= \sigma(B_t(T_1) - B_t(T_2))f(t, r_t, \theta_t) dW^{\mathbb{Q}^{T_1,1}} + \eta(C_t(T_1) - C_t(T_2))f(t, r_t, \theta_t) dW^{\mathbb{Q}^{T_1,2}} \\
&= \sigma(B_t(T_1) - B_t(T_2))X_t dW^{\mathbb{Q}^{T_1,1}} + \eta(C_t(T_1) - C_t(T_2))X_t dW^{\mathbb{Q}^{T_1,2}}
\end{aligned}$$

Since  $W^{\mathbb{Q}^{T_1,1}}$  and  $W^{\mathbb{Q}^{T_1,2}}$  are independent,  $dW^{\mathbb{Q}^{T_1,1}} dW^{\mathbb{Q}^{T_1,2}} = 0$ . So, we know that

$$d[X, X]_t = \sigma^2(B_t(T_1) - B_t(T_2))^2 X_t^2 dt + \eta^2(C_t(T_1) - C_t(T_2))^2 X_t^2 dt$$

Let  $Y_t = \log X_t$ , so we have:

$$\begin{aligned}
dY_t &= \frac{1}{X_t} dX_t - \frac{1}{2} \frac{1}{X_t^2} d[X, X]_t \\
&= \frac{1}{X_t} (\sigma(B_t(T_1) - B_t(T_2))X_t dW^{\mathbb{Q}^{T_1,1}} + \eta(C_t(T_1) - C_t(T_2))X_t dW^{\mathbb{Q}^{T_1,2}}) \\
&\quad - \frac{1}{2} \frac{1}{X_t^2} (\sigma^2(B_t(T_1) - B_t(T_2))^2 X_t^2 dt + \eta^2(C_t(T_1) - C_t(T_2))^2 X_t^2 dt) \\
&= \sigma(B_t(T_1) - B_t(T_2))dW^{\mathbb{Q}^{T_1,1}} + \eta(C_t(T_1) - C_t(T_2))dW^{\mathbb{Q}^{T_1,2}} \\
&\quad - \frac{1}{2} (\sigma^2(B_t(T_1) - B_t(T_2))^2 dt + \eta^2(C_t(T_1) - C_t(T_2))^2 dt)
\end{aligned}$$



$$\begin{aligned}
\Rightarrow Y_{T_1} - Y_t &= \int_t^T \sigma(B_s(T_1) - B_s(T_2))dW^{\mathbb{Q}^{T_1,1}} + \int_t^T \eta(C_s(T_1) - C_s(T_2))dW^{\mathbb{Q}^{T_1,2}} \\
&\quad - \frac{1}{2} \left( \int_t^T \sigma^2(B_s(T_1) - B_s(T_2))^2 ds + \int_t^T \eta^2(C_s(T_1) - C_s(T_2))^2 ds \right) \\
\Rightarrow X_{T_1} &= X_t \exp \left( -\frac{1}{2} \left( \int_t^T \sigma^2(B_s(T_1) - B_s(T_2))^2 ds + \int_t^T \eta^2(C_s(T_1) - C_s(T_2))^2 ds \right) \right. \\
&\quad \left. + \int_t^T \sigma(B_s(T_1) - B_s(T_2))dW^{\mathbb{Q}^{T_1,1}} + \int_t^T \eta(C_s(T_1) - C_s(T_2))dW^{\mathbb{Q}^{T_1,2}} \right)
\end{aligned}$$

Since  $dW^{\mathbb{Q}^{T_1,1}}dW^{\mathbb{Q}^{T_1,2}} = 0$ , we know that

$$\begin{aligned}
&\left( \int_t^T \sigma(B_s(T_1) - B_s(T_2))dW^{\mathbb{Q}^{T_1,1}} + \int_t^T \eta(C_s(T_1) - C_s(T_2))dW^{\mathbb{Q}^{T_1,2}} \right)^2 \\
&= \int_t^T \sigma^2(B_s(T_1) - B_s(T_2))^2 ds + \int_t^T \eta^2(C_s(T_1) - C_s(T_2))^2 ds = \Omega
\end{aligned}$$

So, we have that

$$X_{T_1} \stackrel{d}{=} X_t \exp \left( -\frac{1}{2} \Omega^2 + \Omega Z \right)$$

where  $\Omega^2 = \sigma^2 \int_t^{T_1} (B_s(T_1) - B_s(T_2))^2 ds + \eta^2 \int_t^{T_1} (C_s(T_1) - C_s(T_2))^2 ds$ , and  $Z$  is a standard normal random variable under measure  $\mathbb{Q}^{T_1}$ .

By Black-Scholes, we know that

$$\mathbb{E}_t^{\mathbb{Q}^{T_1}} [(X_{T_1} - K)_+] = X_t \Phi(d_+) - K \Phi(d_-)$$

where  $d_{\pm} = \frac{\log(\frac{P_t(T_2)}{K P_t(T_1)}) \pm \frac{1}{2} \Omega^2}{\Omega}$

Finally, we continue to calculate the price of this option under  $\mathbb{Q}^{T_1}$ .

$$\begin{aligned}
v_t &= P_t(T_1) \mathbb{E}_t^{\mathbb{Q}^{T_1}} [(X_{T_1}(T_2) - K)_+] \\
&= P_t(T_1) (X_t \Phi(d_+) - K \Phi(d_-)) \\
&= P_t(T_1) \frac{P_t(T_2)}{P_t(T_1)} \Phi(d_+) - P_t(T_1) K \Phi(d_-) \quad \left( X_t = \frac{P_t(T_2)}{P_t(T_1)} \right) \\
&= P_t(T_2) \Phi(d_+) - P_t(T_1) K \Phi(d_-)
\end{aligned}$$

Therefore, we can conclude that:

$$v_t = P_t(T_2) \Phi(d_+) - P_t(T_1) K \Phi(d_-)$$

where

$$\begin{aligned}
d_{\pm} &= \frac{1}{\Omega} \log \left( \frac{P_t(T_2)}{K P_t(T_1)} \right) \pm \frac{1}{2} \Omega \\
\Omega^2 &= \sigma^2 \int_t^{T_1} (B_s(T_1) - B_s(T_2))^2 ds + \eta^2 \int_t^{T_1} (C_s(T_1) - C_s(T_2))^2 ds
\end{aligned}$$

#### 2.4. Interest Rate Swap Rate.

An interest rate is an agreement between two parties to exchange cash flows generated by interest payments over fixed period of time. Under no-arbitrage condition, the value of an interest rate swap's fixed leg has to equal to the value of the floating leg. The payments between the two parties of the agreement are propotional to the notional amount  $N$  and the tenors  $\tau_k$ .

Denote the swap rate as  $F$  such that the floating leg and fixed leg have the same value.

##### Fixed leg

The value of the fixed leg is calculated by discounting all the fixed cashflows to the present time using the bond prices:

$$V_t^{\text{Fix}} = NF \sum_{k=1}^n P_t(\tau_k) \Delta \tau_k$$

##### Floating leg

Each floating payment is the multiply of notional amount times, elapsed time and the corresponding forward rate at the time of the previous payment. So, the payment of the floating leg can be expressed as  $N(P_t(\tau_{k-1}) - P_t(\tau_k))$ . Therefore the floating leg value is:

$$V_t^{\text{Float}} = N(P_t(\tau_0) - P_t(\tau_n))$$

Equating the value of two legs, the value of the swap rate at time  $t$  can be written as

$$S_t = \frac{P_t(\tau_0) - P_t(\tau_n)}{\sum_{k=1}^n P_t(\tau_k) \Delta \tau_k}$$

#### 2.5. Interest Rate Swaption Price.

An interest rate swaption is a type of option, which gives the holder the right but not the obligation to enter into an interest rate swap at maturity time  $T$  with strike rate  $K$ . The payoff function of a payer swaption is  $\varphi = 1\{S_T > K\} \cdot (V_T^{\text{Float}} - V_t^{\text{Fix}})$ . When the notional amount is 1 and the payments is periodic, we can write the payoff as below function.

$$V_T = (S_T - F)_+ A_T$$

where

$$A_T = \sum_{m=1}^n P_T(\tau_m) \Delta \tau_m$$

$A_T$  is an annuity and can be used as a numeraire to write the value of a swaption as

$$V_t = A_t \cdot E_t^{\mathbb{Q}_A}[(S_T - F)_+]$$

$$V_t = E_t^{\mathbb{Q}_B}[e^{-\int_t^T r_s ds} (S_T - F)_+ A_T]$$

Since  $S_T = \frac{P_T(\tau_0) - P_T(\tau_n)}{(\tau_n)}$ , we can observed that the  $S_T$  is a relative to the numeraire asset. Under the  $\mathbb{Q}_A$  measure,  $S_T$  is a martingale, thus the lognormal swap rate model can be constructed based on considering the swap rate process as a lognormal process under this measure.

## 2.6. Implied volatility.

Recall that under Lognormal Swap Rate Model (LSM), interest rates  $\beta = (\beta)_{t \geq 0}$  are assumed to be deterministic and asset price are assumed to satisfies the following  $\mathbb{Q}_A$  dynamic.

$$S_T = S_t \exp \left( -\frac{1}{2} \int_t^T \beta_u^2 du + \int_t^T \beta_u dW_u^{\mathbb{Q}_A} \right)$$

$$S_T \stackrel{d}{=} S_t \exp \left( -\frac{1}{2} \Omega^2 + \Omega Z \right)$$

where  $Z \stackrel{\mathbb{Q}_A}{\sim} N(0, 1)$ ,  $\Omega = \left( \int_t^T \beta_u^2 du \right)^{\frac{1}{2}}$  hence  $S_T|_{F_t}$  can be simulated as below:

$$V_t = A_t [S_t \Phi(d_+) - K \Phi(d_-)]$$

where

$$d_{\pm} = \frac{1}{\Omega} \times (\log(S_t/K) \pm \frac{1}{2} \Omega^2)$$

We would be able to see that it is in the format of a Black-Scholes Model when setting  $r = 0$  and  $\sigma = \frac{\Omega}{\sqrt{T-t}}$ .

Let  $V^{LSM}(K, T, S_0, r = 0, \sigma)$  be the LSM model-implied swaption price for a given set of parameters and let  $V^*(K, T, S_0)$  be the simulated price of the same option. Implied volatility,  $\sigma_{\text{imp}}$  is the value of the  $\sigma$  that equates the two prices:

$$V^{LSM}(K, T, S_0, r = 0, \sigma) = V^*(K, T, S_0)$$

Here, having fixed tenure structure  $\tau = \{3; 3.25; \dots; 6\}$ , the swaption is having fixed maturity. So the implied volatility can be viewed as a function of strike. Varying  $K$  and plotting the resulting implied volatility value yields an implied volatility (IV) curve.

Given the assumption that the strike is equal to today's swap-rate (i.e.  $K = S_0$ ). To check the result for a collection of strikes  $\alpha * K$  where  $\alpha = 0.95, 0.96, \dots, 1.05$ , we have

$$V_0 = A_0 [S_0 \Phi(d_+) - \alpha K \Phi(d_-)]$$

$$\frac{V_0}{A_0 S_0} = \Phi(d_+) - \Phi(d_-)$$

$$d_{\pm} = \frac{1}{\Omega} \times (-\log(\alpha) \pm \frac{1}{2} \Omega^2)$$

Therefore the implied volatility can be derived using Brutal Force algorithm equating  $\frac{V_0}{A_0 S_0}$  and  $\Phi(d_+) - \Phi(d_-)$ .

### 3. Results

#### 3.1. Base Case Assumptions.

To implement the analysis, we set up a specific base case to work on, where we implemented sensitivity and scenario analysis to explore the effect of long and short-term model factors, including mean-reversion rate and volatility, on the investment products (bond, bond option, and swaption) mentioned in previous sections.

Model Parameters	Base Value
Current Short-term rate	$r_0 = 2\%$
Mean reversion rate	$\alpha = 3$
Short-term volatility	$\sigma = 1\%$
Current Long-term rate	$\theta_0 = 3\%$
Mean reversion rate	$\beta = 1$
Mean reversion level	$\phi = 5 \%$
Long-term volatility	$\eta = 0.5\%$

**Four scenarios of the current long and short term interest rate** are investigated when changing the model parameters, by assuming the current  $r_0, \theta_0$  higher or lower than the mean-reversion level  $\phi = 0.05$ . Four cases are base case ( $r_0=0.02, \theta_0 = 0.03$ ), high current short-term rate ( $r_0=0.1, \theta_0 = 0.03$ ), high current long-term rate ( $r_0=0.02, \theta_0 = 0.1$ ), and high current long and short-term rate ( $r_0 = \theta_0 = 0.1$ ).

### 3.2. Bond Yield under Different Scenarios.

In the base case, we used an **Euler-scheme** to simulate 1000 long and short run interest rates paths and used these paths to generate the bond yields by using Monte Carlo estimation. From the following graph (Figure 3), we can find that the **simulated bond yields matched the results obtained by the analytical formula**, and the confidence bands of the simulations are closed to the analytical results. Therefore, analysts can use the analytical formula to investigate the bond yield behavior under different scenarios. Figure 4 - 6 investigate **four scenarios of the current long and short term interest rate**, and the results are as follows:

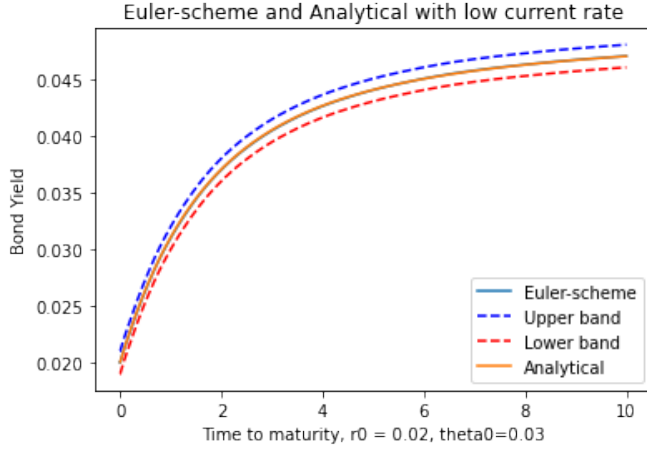


FIGURE 3. **Base Case:** Simulated and Analytical,  $r_0=0.02$ ,  $\theta_0 = 0.03$

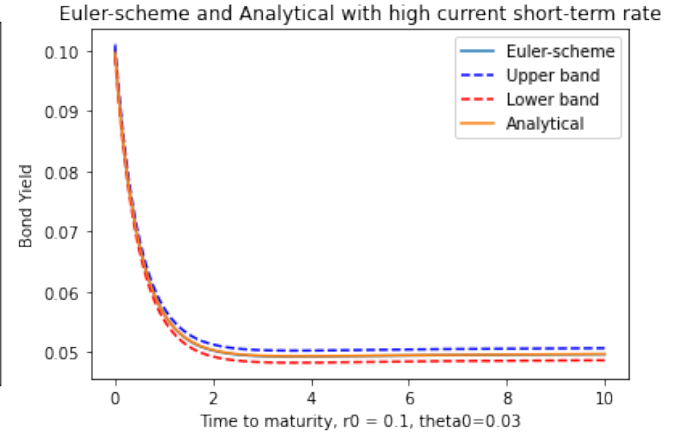


FIGURE 4. Simulated and Analytical Bond Yield  $r_0=0.1$ ,  $\theta_0 = 0.03$

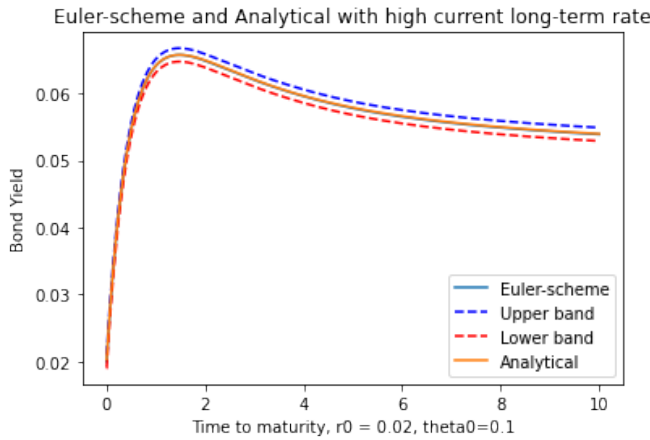


FIGURE 5. Simulated and Analytical Bond Yield  $r_0=0.02$ ,  $\theta_0 = 0.1$

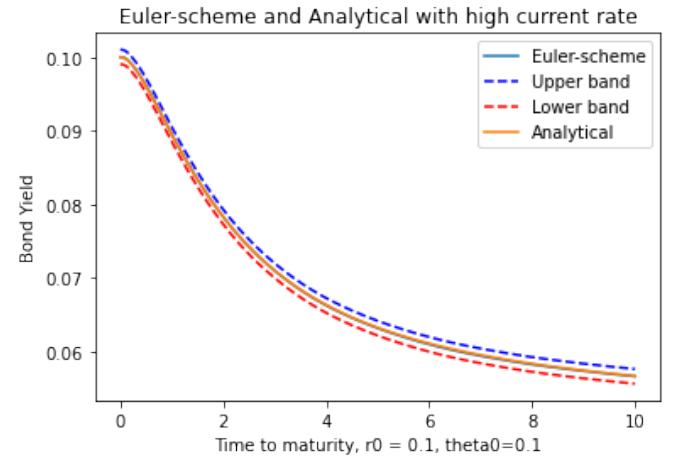


FIGURE 6. Simulated and Analytical Bond Yield  $r_0 = \theta_0 = 0.1$

Figure 3 shows the base case, if the current interest rate is lower than the long-term reversion level, the bond yield increases as the time to maturity increases, with decreasing growth rate. At maturity = 0, the bond yield is the current spot rate =  $r_0 = 0.02$ . As the maturity increase to 10, the bond yield

reached to 0.05 ( $=\phi$ ). On the contrary, if the current interest rate is higher than the long-term reversion level ( $r_0 = \theta_0 = 0.1$ ), the bond yield decrease as the time to maturity increases, and it will eventually reach to  $\phi = 0.05$  with a lower decreasing speed. As long as the current short-term rate higher than the reversion level, the bond yield have positive convexity, and vise versa. By fixing a high current short-term rate ( $r_0 = 0.1$ ), the higher the current long-term interest rate, the smaller the convexity.

Additionally, with a low current short-term rate and a high current long-term rate, the convexity of the bond yield will be negative for some small maturity and went to slightly positive as maturity increase, which showed in Figure 5. Since the model assume the short-term rate approaches to the long-term rate, under a high  $\theta_0 = 0.1$  The bond yield will rise sharply at low maturity, and then be pulled back to 0.05 by the long-term mean reversion level.

### 3.2.1 Drift term parameter corresponding with dt

Based on the interest rate model assumptions, we first compared the parameters related to drift term under four different current interest rate scenarios.

#### a.) Analytical comparison of short-term reversion speed $\alpha$

Based on the figure 7 and 9, increase the short-term mean-reversion speed  $\alpha$  increase the curvature of the yield and drives a higher Bond Yield. It can be seen that different bond yields are combined to form an olive shape. When maturity = 0, or maturity is long enough, bond yield converges to the long-term mean-reversion level  $\phi$ . If we start from a lower level (0.02) interest rate point, for the maturity of the middle segment, the faster the interest rate returns to the mean value (0.05), the faster the interest rate raise, so we have a lower bond price and a higher bond yield. Changing the short-term mean-reversion speed has a relatively small impact on bond yield, because short-term interest rates will eventually be suppressed by the long-term mean-reversion level and long-term mean-reversion speed.

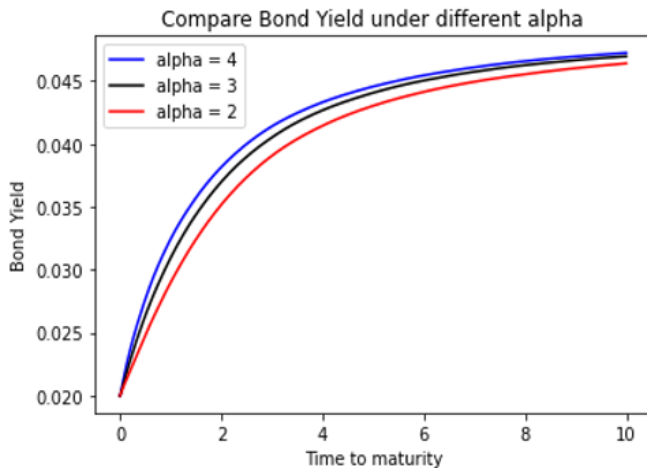


FIGURE 7. Analytical Compare parameter  $\alpha$ ,  $r_0 = 0.02$ ,  $\theta_0 = 0.03$

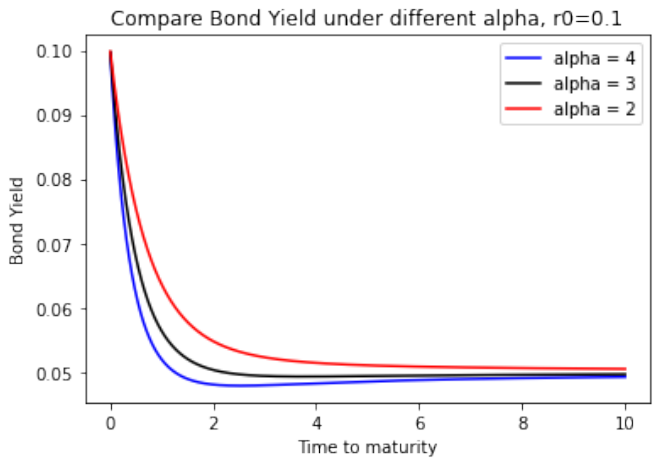


FIGURE 8. Analytical Compare parameter  $\alpha$ ,  $r_0 = 0.1$ ,  $\theta_0 = 0.03$

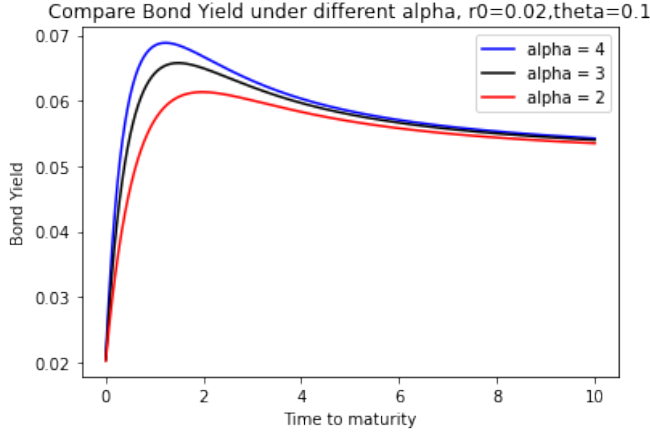


FIGURE 9. Analytical Compare parameter  $\alpha$ ,  $r_0 = 0.02$ ,  $\theta_0 = 0.1$

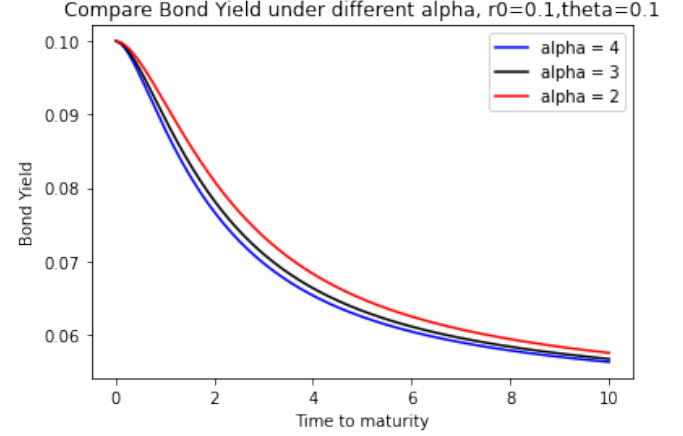


FIGURE 10. Analytical Compare parameter  $\alpha$ ,  $r_0 = 0.1$ ,  $\theta_0 = 0.1$

Next, if we current start at a high short-term rate ( $r_0=0.1$ ), the current bond price is low. The higher the  $\alpha$  means the interest rate decrease faster, which implies a higher bond price and lower bond yield. This can be observed in Figure 8 and 10, for both case where  $r_0 = 0.1, \theta_0 = 0.03$  and  $r_0 = 0.1, \theta_0 = 0.1$ . The bond yield converge to  $\phi = 0.05$ , which is same as the other two cases.

b.) Analytical comparison of long-term reversion speed  $\beta$

Similarly, Figure 11-14 also shows a olive shape. We can expect the bond yield will converge to a single value around 0.05 ( $=\phi$ ) for some time to maturity over 10 years. When the yield curve has negative convexity (Figure 11 and 13), increase the long-term mean-reversion speed  $\beta$  increase the absolute value of the yield curve curvature and drives a higher Bond Yield rate. Comparing to  $\alpha$ , bond yield is more sensitive to  $\beta$ , as increase the same level of  $\beta$ , the shape change of bond yield is more significant.

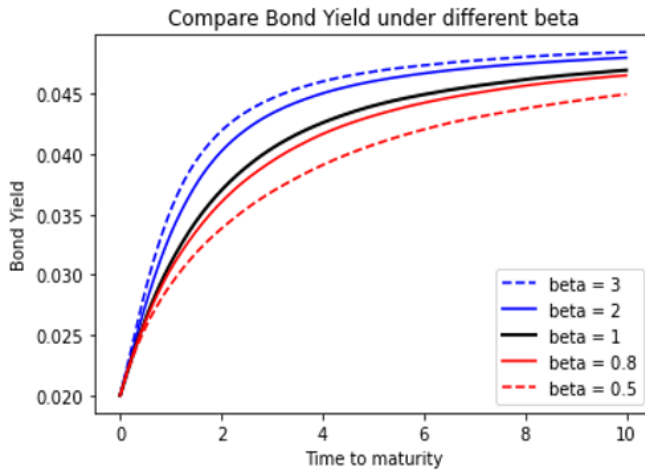


FIGURE 11. Analytical Compare parameter  $\beta$ ,  $r_0 = 0.02$ ,  $\theta_0 = 0.03$

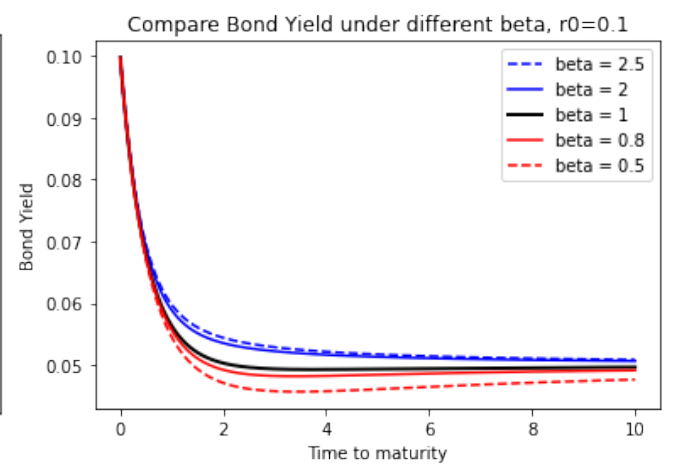


FIGURE 12. Analytical Compare parameter  $\beta$ ,  $r_0 = 0.1$ ,  $\theta_0 = 0.03$

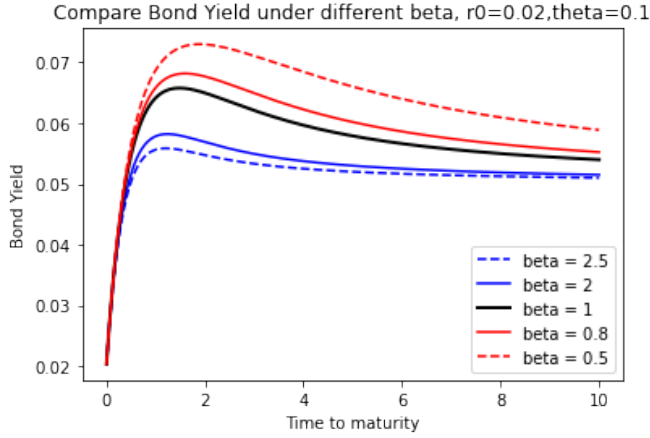


FIGURE 13. Analytical Compare parameter  $\beta, r_0 = 0.02, \theta_0 = 0.1$

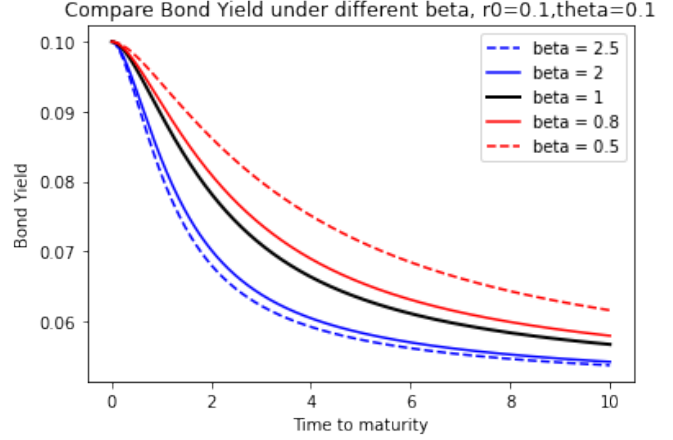


FIGURE 14. Analytical Compare parameter  $\beta, r_0 = 0.1, \theta_0 = 0.1$

When the yield curve has positive convexity (Figure 12 and 14), increase the long-term mean-reversion speed  $\beta$  also increase the absolute value of the yield curve curvature and drives a lower Bond Yield rate. This can be explained using the same logic as we explain the impact of various  $\alpha$ . If the current interest rate is higher than the reversion level, decreasing the speed of the long-term reversion means the ongoing future interest rate remaining at a high level, which leads to a lower bond value and higher bond yield, such as the  $\beta = 0.5$  case in Figure 14. Additionally, if the current interest rate is lower than the reversion level, increasing the speed of the long-term reversion leads to a lower bond value and higher bond yield, such as the  $\beta = 3$  case in Figure 11. It is because the future interest rate increase faster to reach the higher reversion level 0.05.

c.) Analytical comparison of mean-reversion level  $\phi$

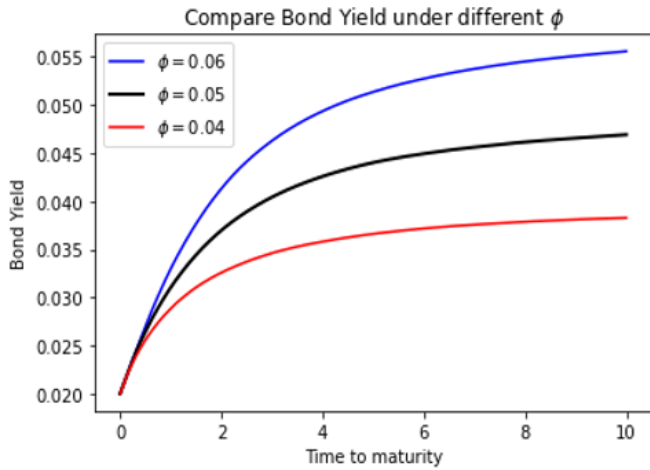


FIGURE 15. Analytical Compare parameter  $\phi, r_0 = 0.02, \theta_0 = 0.03$

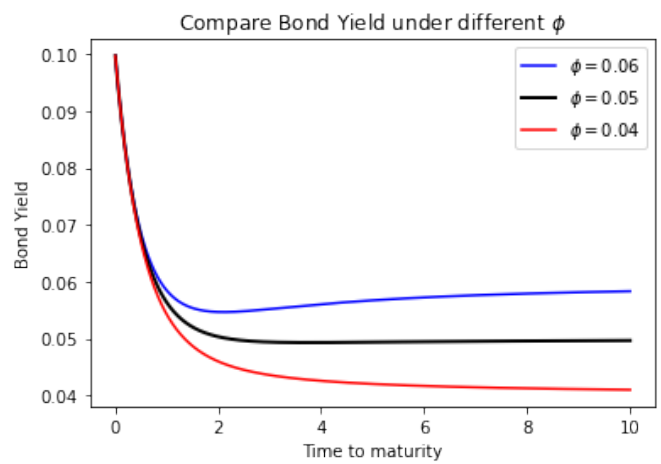


FIGURE 16. Analytical Compare parameter  $\phi, r_0 = 0.1, \theta_0 = 0.03$



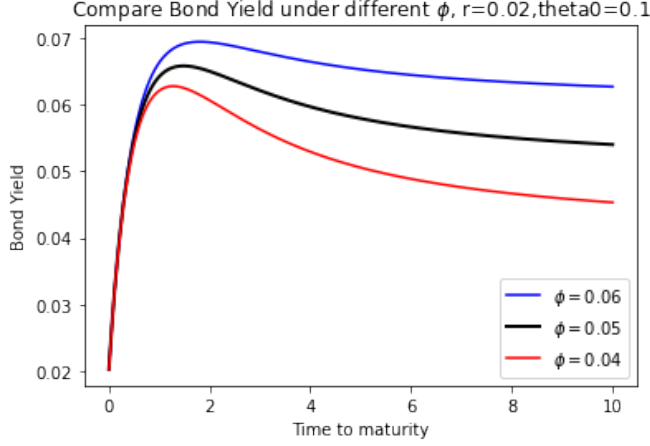


FIGURE 17. Analytical Compare parameter  $\phi$ ,  $r_0 = 0.02$ ,  $\theta_0 = 0.1$

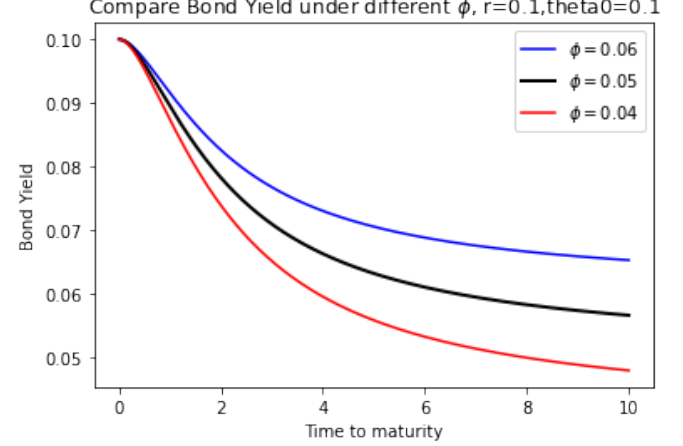


FIGURE 18. Analytical Compare parameter  $\phi$ ,  $r_0 = 0.1$ ,  $\theta_0 = 0.1$

Finally, Figure 15-18 implies that for all the interest rate scenarios, as the maturity increase the bond yield will eventually converge to the long-term mean-reversion level  $\phi$ . When keeping the same reversion speed, the curvature of the curve have no significant change. When the yield curve decrease, increasing  $\phi$  can reduce the steepness of the curve and vice versa. The bond yield curve is very sensitive to the value of long-term reversion level as it determine the bond yield converge level as maturity increase. Overall, we can conclude that the **change of  $\alpha$  and  $\beta$**  can change the **curvature** of the bond yield, while the **change of  $\phi$**  can change the **level** of the bond yield curve.

#### d.) Compare Euler-scheme and Analytical Bond Yield under extreme scenarios

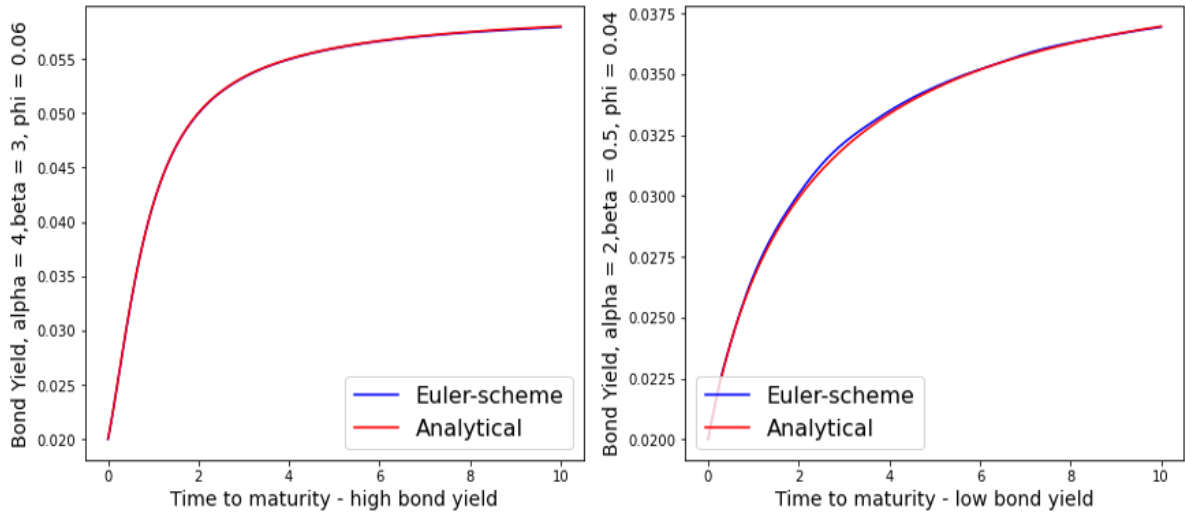


FIGURE 19. Euler-scheme Simulation Accuracy under High and Low Bond Yield

In order to test the accuracy of the Euler-scheme simulation to support subsequent research, we changed the drift-related parameters in the model for testing. Under the base case interest scenario, for the high

yield case, we set  $\alpha = 4, \beta = 3$  and  $\phi = 0.06$ , and for the low yield case, we set  $\alpha = 2, \beta = 0.5$  and  $\phi = 0.04$ . The results show that changing  $\alpha, \beta$  and  $\phi$  will not affect the accuracy of the simulation, as the interest rate process is a Q-martingale.

### 3.2.2 Volatility parameter corresponding with dWt

a.) Analytical comparison of short-term volatility  $\sigma$

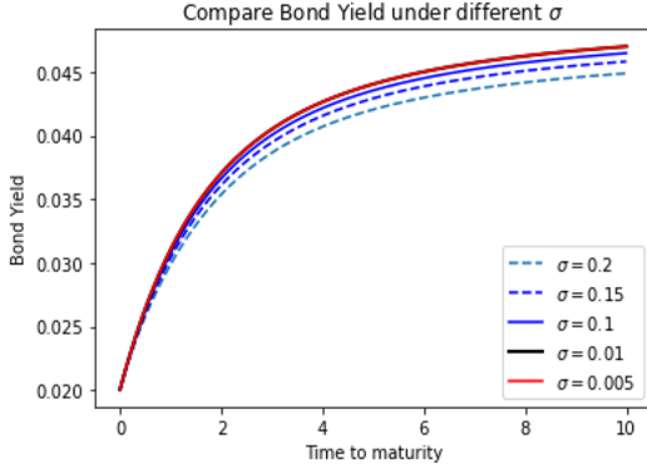


FIGURE 20. Analytical Compare parameter  $\sigma, r_0 = 0.02, \theta_0 = 0.03$

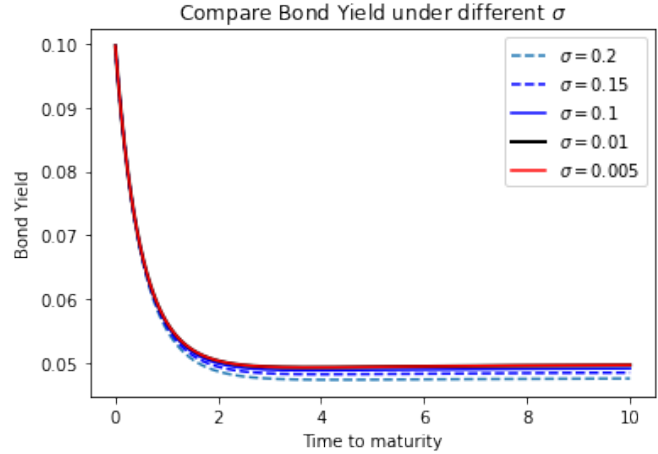


FIGURE 21. Analytical Compare parameter  $\sigma, r_0 = 0.1, \theta_0 = 0.03$

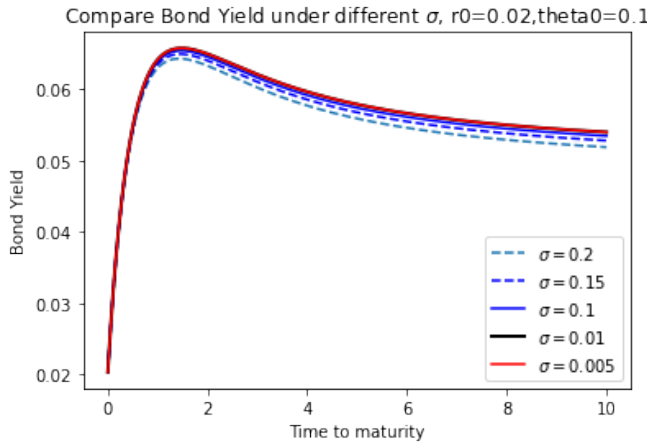


FIGURE 22. Analytical Compare parameter  $\sigma, r_0 = 0.02, \theta_0 = 0.1$

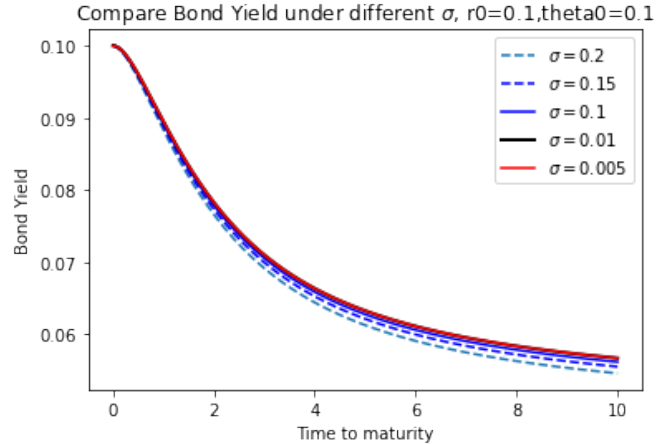


FIGURE 23. Analytical Compare parameter  $\sigma, r_0 = 0.1, \theta_0 = 0.1$

Bond investor benefit from higher short-term volatility, therefore increasing in  $\sigma$  can increase the bond price and leads to lower bond yield curve for all four scenarios. As the maturity increase, the the uncertainty increase, so that the yield is more sensitive to the change of volatility. However, the influence of the short-term volatility on the yield curve is small. Bond investor is hard to get large benefit from taking the short-term volatility.

b.) Analytical comparison of long-term volatility  $\eta$

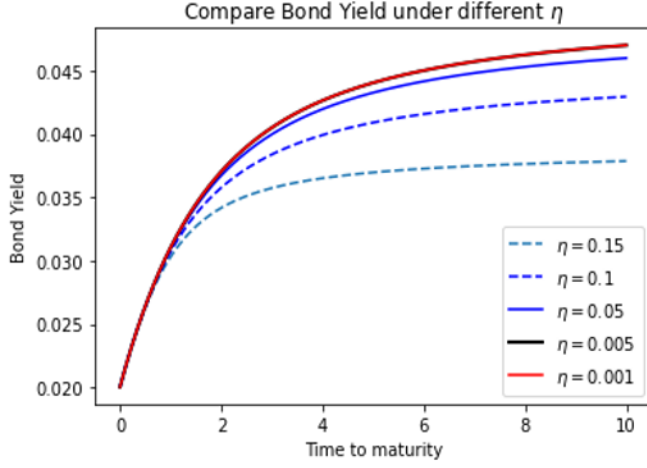


FIGURE 24. Analytical Compare parameter  $\eta$ ,  $r_0 = 0.02$ ,  $\theta_0 = 0.03$

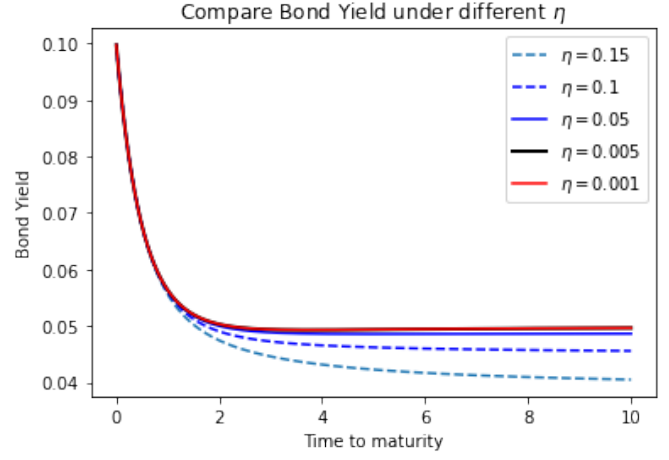


FIGURE 25. Analytical Compare parameter  $\eta$ ,  $r_0 = 0.1$ ,  $\theta_0 = 0.03$

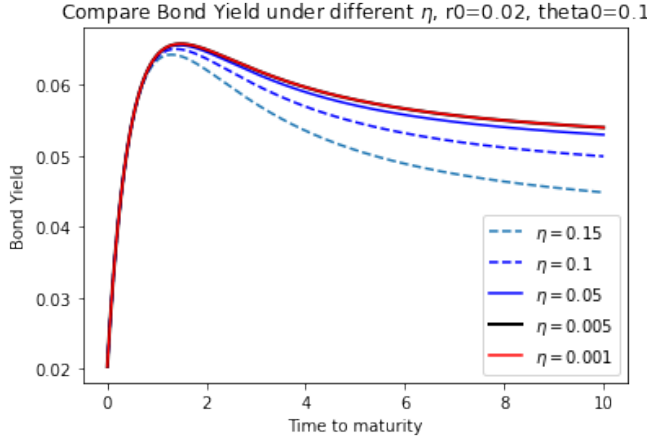


FIGURE 26. Analytical Compare parameter  $\eta$ ,  $r_0 = 0.02$ ,  $\theta_0 = 0.1$

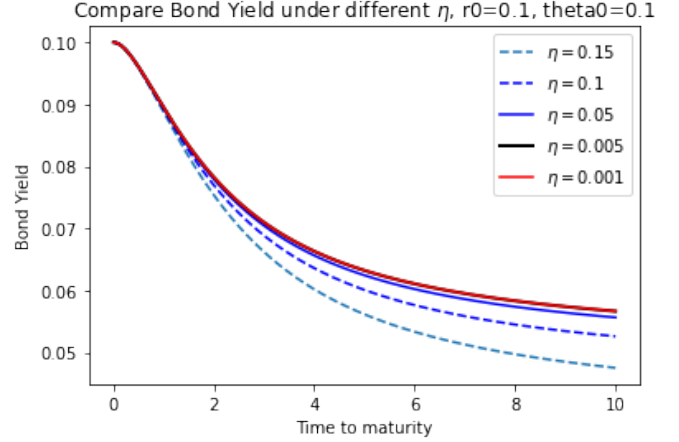


FIGURE 27. Analytical Compare parameter  $\eta$ ,  $r_0 = 0.1$ ,  $\theta_0 = 0.1$

Similarly, increasing in the long-term volatility  $\eta$  can significantly increase the bond price and leads to lower bond yield curve for all four scenarios. We can see from the curve that the bond price no longer converge to the long-term mean-reversion level ( $\phi = 0.05$ ) if the volatility is large enough. As the maturity increase, the increasing uncertainty makes the yield more sensitive to the change of volatility. Bond investor have the opportunity to get large compensation from taking the long-term volatility. Meanwhile, investors can use different investment product, such as bond option and swaption, to hedge the interest rate uncertainty.

c.) Compare Euler-scheme and Analytical Bond Yield under different volatility

Alternatively, we tried simulate bond yield curve using different long and short-term volatility ( $\sigma, \eta$ ). We found that the simulation accuracy decrease as volatility-related parameter increase. Based on the figure below, the simulated yield curve fluctuated when the volatility is high ( $\sigma=0.2, \eta=0.15$ ).

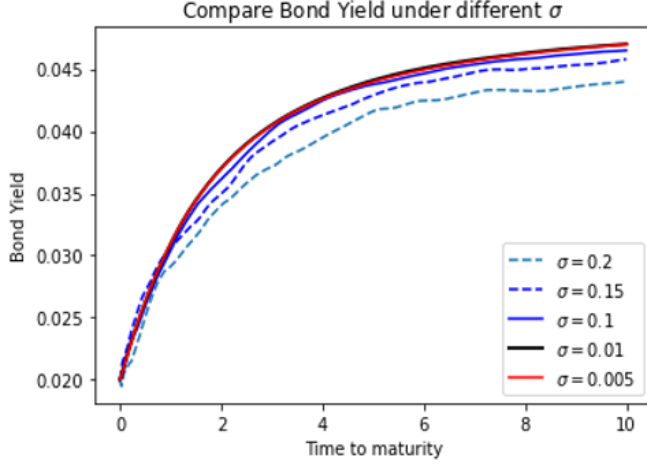


FIGURE 28. Simulated Yield under different  $\sigma$

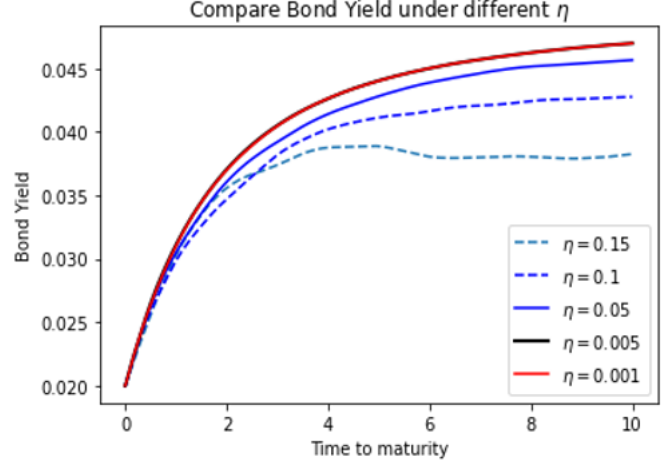


FIGURE 29. Simulated Yield under different  $\eta$

We further investigated the impact of Euler-scheme simulation accuracy by changing in long and short-term volatility separately or together. We find that increasing short-term interest rate volatility has less impact on simulation accuracy than increasing long-term interest rate volatility. Analysts should be aware of the simulation accuracy when investigating yield curve shape under different  $\sigma$  and  $\eta$ . Although there is a trade of between the computational cost and accuracy, it is necessary to reduce the simulation error by using an appropriate simulation times based on the modeling needs.

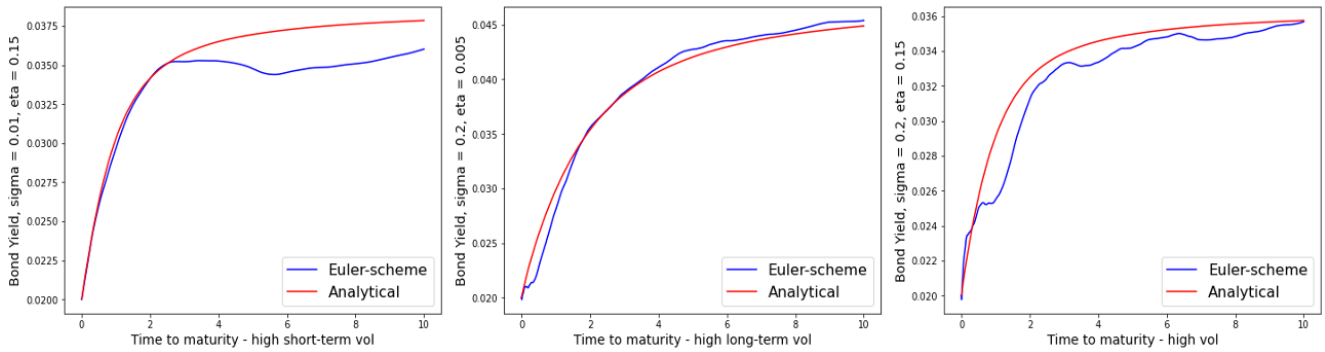


FIGURE 30. Euler-scheme Simulation Accuracy and Volatility

### 3.3. Bond Option.

First, we used Euler-scheme to simulate the interest rate paths under the risk-neutral measure and the forward-neutral measure. Then, we used the simulations of forward-neutral interest rate paths and the analytic expression determined in section 2.3 to calculate the price of the bond option (call option) for some different strikes. Using Monte Carlo simulation under risk-neutral and forward-neutral measures, we generate the price of the bond option for some different strikes. The bond option prices obtained by the previous three approaches are shown in the following graph.

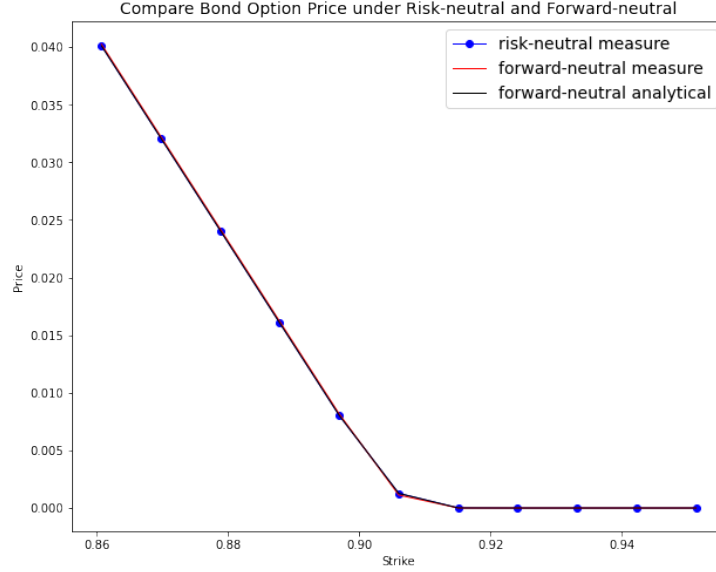


FIGURE 31. Bond Option Price under Different Measure

From the previous graph, we can find that the bond option price under the risk-neutral measure matches the bond option price under the forward-neutral measure. Under forward-neutral measure, the bond option price generated by the analytic expression and Monte Carlo simulation are approximately same. Thus, we can conclude that the bond option price generated by Monte Carlo simulation under the risk-neutral and forward-neutral measures and the analytical formula under forward-neutral are almost same.

Furthermore, since the call option pays  $(\text{bond price when option matures} - \text{strike price})_+$  when it matures, the price of the bond option decreases as the strike increases. If the strike price is so high that it is almost not possible that the bond price is higher than the strike price when the option matures, then the price of the bond option will be zero.

Next, we investigated what the various parameters do to the bond option price using the analytical formula.

a.) Short-term mean reversion speed  $\alpha$  and long-term mean reversion speed  $\beta$

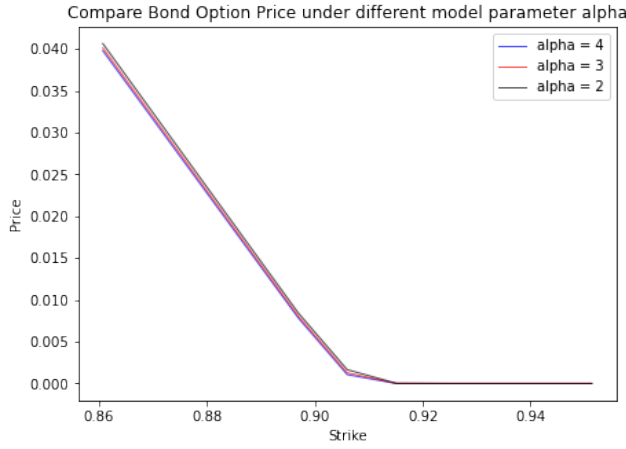


FIGURE 32. Bond Option Price with Different  $\alpha$

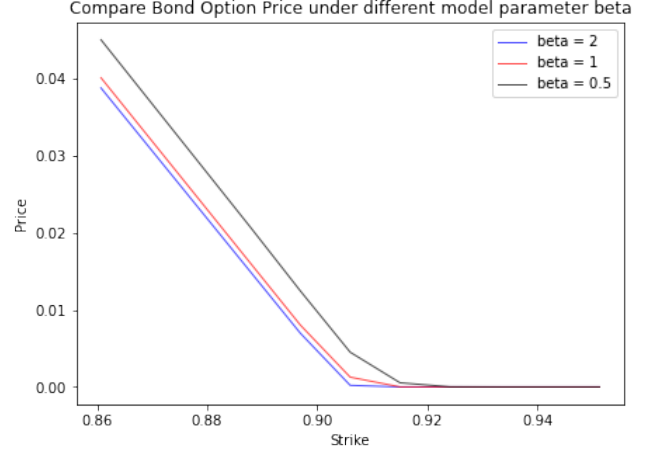


FIGURE 33. Bond Option Price with Different  $\beta$

From the previous graphs, we found that the change of short-term mean reversion speed nearly has no impact on the bond option price. Furthermore, the bond option price is sensitive to long-term mean reversion speed. As the long-term mean reversion speed decreases, the bond option price increases.

b.) Short-term volatility  $\sigma$  and long-term volatility  $\eta$

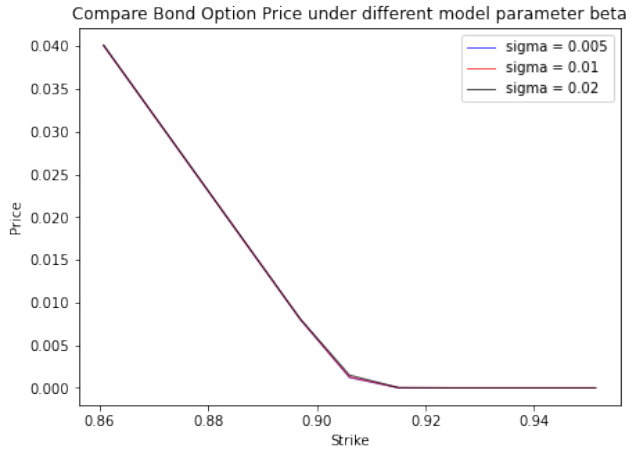


FIGURE 34. Bond Option Price with Different  $\sigma$

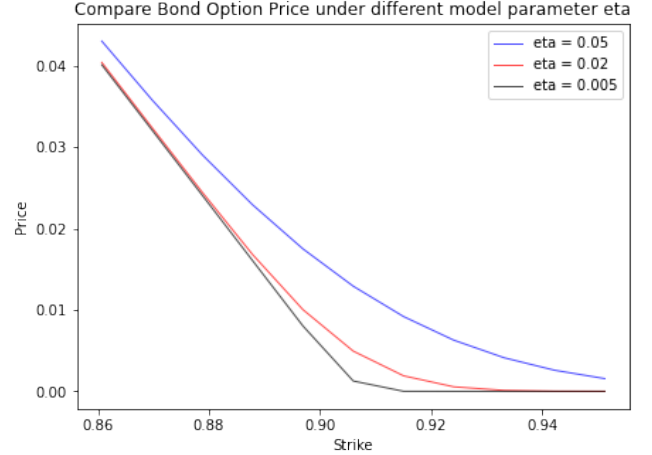


FIGURE 35. Bond Option Price with Different  $\eta$

From the previous graphs, we found that the bond option price is sensitive to the long-term volatility and has no obvious change when the short-term volatility changes. When the long-term volatility increases, the bond option price increases. In details, the change of the bond option price with respect to the long-term volatility is more obvious when the strike price is close to the current market price of the underlying bond.

c.) Option maturity  $T1$  and bond maturity  $T2$

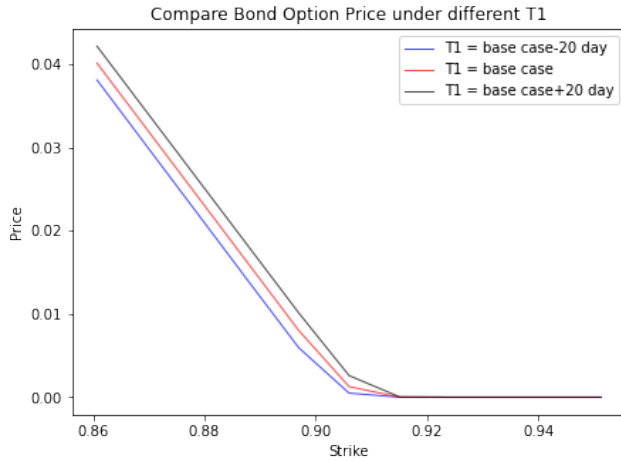


FIGURE 36. Bond Option Price with Different  $T1$

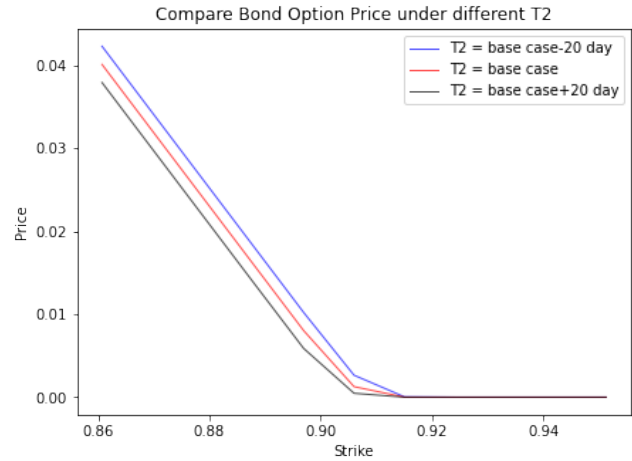


FIGURE 37. Bond Option Price with Different  $T2$

From the previous graphs, we found that the bond option price increases as the maturity of the option increases, and the bond option price increases as the maturity of the bond decreases. The reason is that the investors want the bond mature as soon as possible after they exercise the option, so a smaller gap between the option maturity and the bond maturity leads to a higher bond option price.

### 3.4. Swaption Implied Volatility.

The below investigation and plots are based on the assumption that we have an Interest Rate Swap (IRS) with tenure structure  $\tau = 3, 3.25, \dots, 6$ . The first reset data is at 3, so the payments are made at  $3.25, 3.5, \dots, 5.75, 6$ . As mentioned in the previous sections, the interest rate path can be simulated for the time from 0 to 6.

Then the interest rate paths can be used to generated 1000 estimation of bond prices with maturities  $T = \{0, 0.25, \dots, 5.75, 6\}$ . Then the swap rates for an IRS with maturity  $T_1 = 3$  were calculated with the function provided in the methodology section. Similarly, we predicted the swap rate of a swap with maturity 6. Using the simulated swap rates, the swaption price based on this IRS was generated.

We predicted a collection of swaption prices setting the strike equal to  $0.95S_0, 0.96S_0 \dots 1.05S_0$ . From the figure 38, we can see that the swaption price is a an increasing function of volatility. Which is in line with the theory that the swaption price is a monotonically increasing function of volatility.

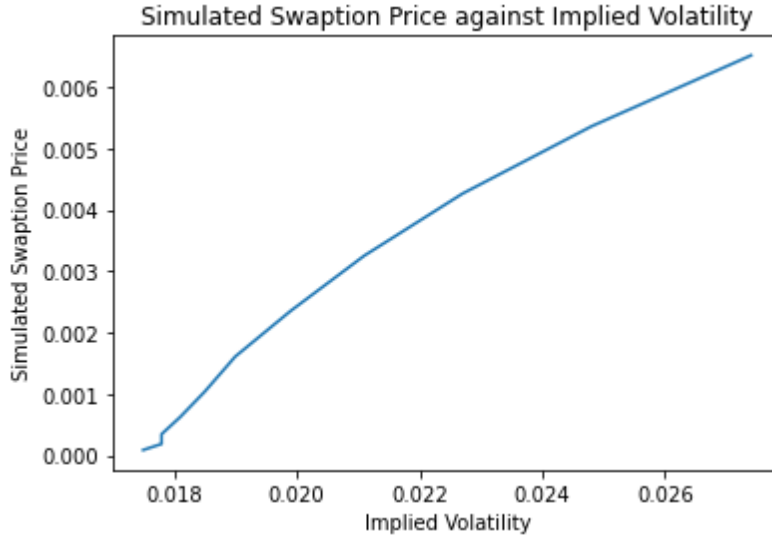


FIGURE 38. Implied volatility's relationship with swaption price

Then we plotted the changing strikes with corresponding implied volatilities to investigate their relationship. The implied volatility smile is a common graph shape when plotting the set of strikes and the implied volatility for options with the same underlying asset and expiration date. In the figure 40 we are able to visualize a shape that is close to a volatility smile. As we reduce the maturity time  $T_1$ , "smile" will be more obvious.

However, the plotted implied volatility curve against strike prices is not always the same shape; it sometimes shows a shape that is closer to a volatility skew, for instance in figure 39. In both cases, we can see from the figures that the IV changes with respect to the strikes. However, the implied volatility might not solely depend on the strikes. From the figure 41, we can see that as the strike goes up, the simulated swaption price decreases, the swaption will change from in-the-money (ITM) to at-the-money (ATM) to out-of-the-money (OTM). The "swaption price"- "strike" dynamics could also impact the implied volatility. Generally, an ITM swaption is more valuable than an OTM swaption which explains the IV is plotted as a curve. In the graph of the IV smile, when the swaption is further



ITM, the IV is higher. When the swaption is deeper OTM, the IV starts to increase slightly. In the graph of the IV skew, the IV is showing a gradually decreasing trend as the strike increases despite the changes from ITM to OTM.

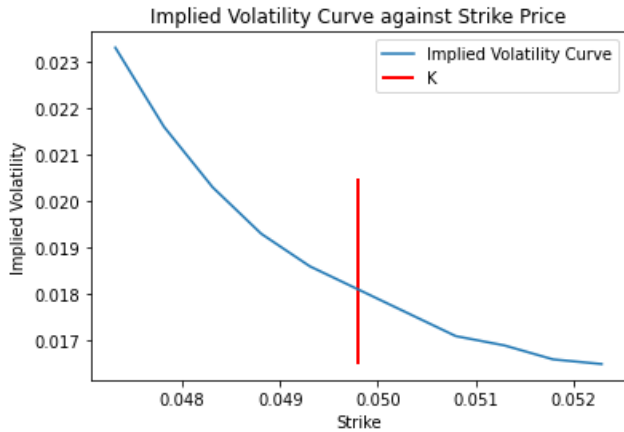


FIGURE 39. Implied Volatility Skew

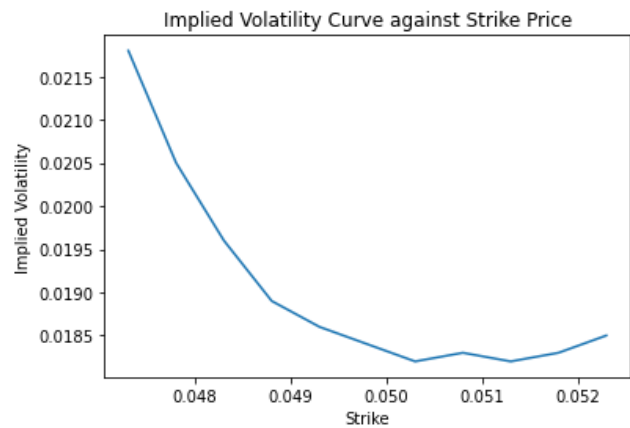


FIGURE 40. Implied Volatility Smile

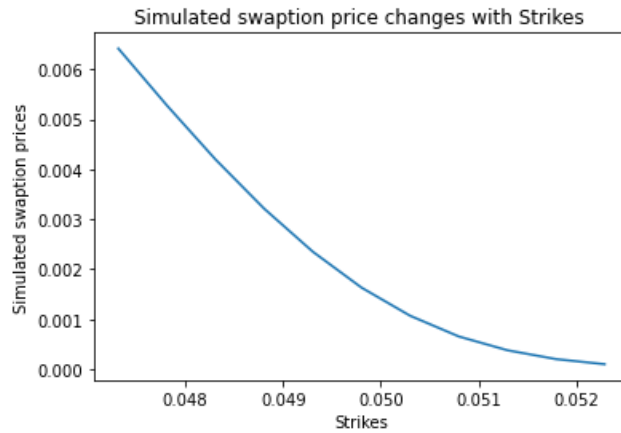


FIGURE 41. Strikes VS Simulated Swaption Prices

The intuitive explanation for the unstable shape of the IV curve is that the swaption prices determined by simulated interest rates are changing with each simulation. As an IRS payer, our payment is based on the fixed rate. For the case that our swaption is more likely to exercise, for instance the generated swap rates at maturity is relatively higher, we would receive a cash flow periodically. The swaption would show similar characteristic to a bond. Hence the IV curve would be more like a volatility smile. On the other hand, when the generated swap rates at maturity is relatively lower than strike, the swaption has less possibility to exercise. Then holding the swaption is similar to holding equity. Therefore the IV curve is more like a volatility skew.

With the two-factor interest rate model, we will be able to change parameters such as  $\alpha, \beta, \phi$  to shift the interest rate path and investigate the influence of simulated swaption prices.

From figure 42 and figure 43, we can see the trend of simulated swaption changes with respect to the strike's scale factors, i.e. the values that we used to multiply to the strike to generate strike sets. These graph shows how the simulated swaption price is affected by the different simulations of short and long rates.

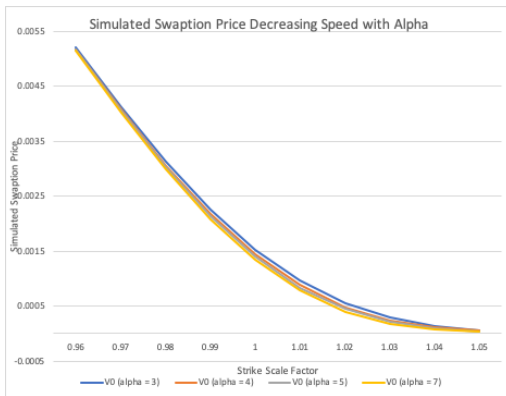


FIGURE 42. Simulated Swaption Price with  $\alpha$



FIGURE 43. Simulated Swaption Price with  $\phi$

a).  $\alpha$ : “mean reversion speed for short rate  $r$ ”.

The figure 44 is a plot of strike's scale factor  $A = 0.95, 0.95 \cdots 1.05$  vs the implied volatility curve corresponding to the  $\alpha$  changes. By observation,  $\alpha$  influence the **curvature** of the IV. Though the changes in the different smiles is not large, we can observe the trend that as  $\alpha$  increases the IV smile shows more curvature and more like a smile. As  $\alpha$  decreases, the curvature decreases as well and the IV curve is more like a skew.

b).  $\beta$ : “mean reversion speed for long rate  $\theta$ ”.

Observing the figure 45, we can see that  $\beta$  influence the **level** of the IV skew. When beta is smaller than 1, a relatively small decrease in  $\beta$  will shift the IV curve up. This could due to the reason that the yield curve is more sensitive to mean reversion speed for long rate. The shape remains almost the same for different  $\beta$ .

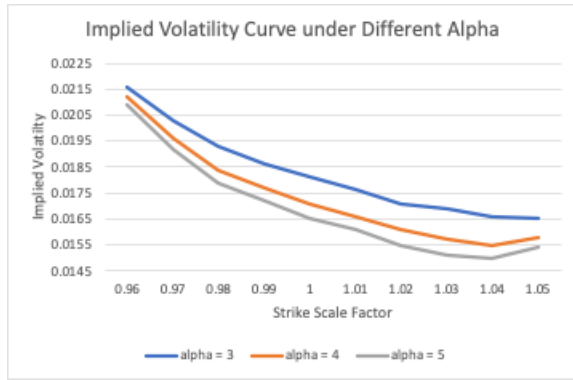


FIGURE 44. Implied Volatility Curve change with  $\alpha$

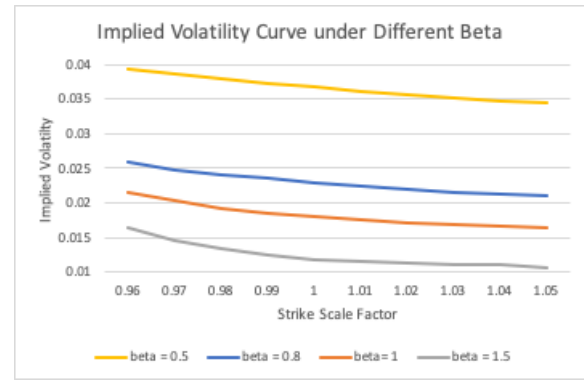


FIGURE 45. Implied Volatility Curve change with  $\beta$

c).  $\phi$ : “mean reversion level for long rate  $\theta$ ”.

This parameter also influence the **level** of the IV skew. As the  $\phi$  goes up, the IV curve shift down. Similar to  $\beta$ , the IV curve’s shape has no significant changes. We know from the previous section that  $\phi$  change the level of the bond yield curve, hence impacting the simulated swap rate and the impact will be eventually reflected on swaption price.

d).  $\sigma$ : “instantaneous volatility for short rate  $r$ ”.

This parameter also influence the **level** of the IV skew. As the  $\sigma$  goes up, the IV curve shift upward. Similarly, the IV curve’s shape has no significant changes. As discussed in the previous chapters, the  $\sigma$  increases will decrease the yield curve and push up the bond prices. As a result, the investors could also benefit from the volatility in terms of a swaption reflected as higher implied volatility. In the mean time, the interest rate risk should not be ignore.

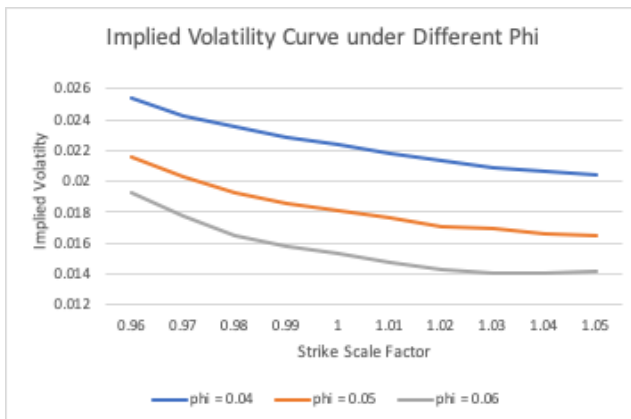


FIGURE 46. Implied Volatility Curve change with  $\phi$

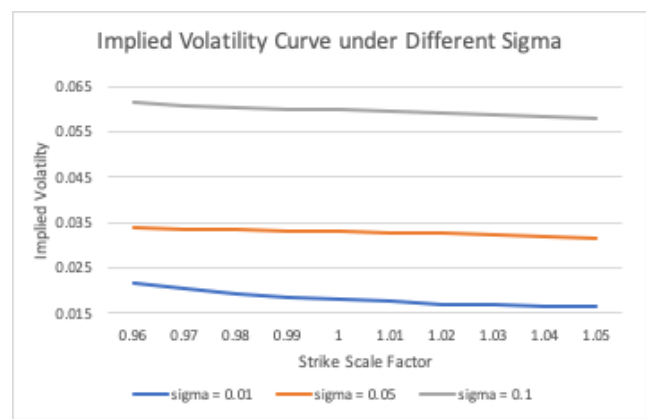


FIGURE 47. Implied Volatility Curve change with  $\sigma$

#### 4. Conclusion

In conclusion, assuming a two factor interest rate model, bond price process can be expressed as a deterministic function. Therefore, we can conclude that the bond price process is

$$P_t(T) = \exp(A_t(T) - B_t(T)r_t - C_t(T)\theta_t)$$

where

$$\left\{ \begin{array}{l} A_t(T) = \frac{1}{2}\sigma^2 D - \beta\phi E + \frac{1}{2}\eta^2 F \\ D = \frac{1}{\alpha^2}[(T-t) + \frac{1}{\alpha}(-\frac{3}{2} + 2e^{-\alpha(T-t)} - e^{-2\alpha(T-t)})] \\ E = \frac{T-t}{\beta} + \frac{\alpha}{\alpha-\beta}(\frac{1-e^{-\alpha(T-t)}}{\alpha^2} - \frac{1-e^{-\beta(T-t)}}{\beta^2}) \\ F = \frac{T-t}{\beta^2} + \frac{1-e^{-2\alpha(T-t)}}{2\alpha(\alpha-\beta)^2} + \frac{2(1-e^{-\alpha(T-t)})}{\alpha\beta(\alpha-\beta)} - \frac{2\alpha(1-e^{-(\alpha+\beta)(T-t)})}{(\alpha-\beta)^2\beta(\alpha+\beta)} - \frac{2\alpha(1-e^{-\beta(T-t)})}{(\alpha-\beta)\beta^3} + \frac{\alpha^2(1-e^{-2\beta(T-t)})}{2(\alpha-\beta)^2\beta^2} \\ B_t(T) = \frac{1-e^{-\alpha(T-t)}}{\alpha} \\ C_t(T) = \frac{\alpha}{\alpha-\beta}(\frac{1-e^{-\beta(T-t)}}{\beta} - \frac{1-e^{-\alpha(T-t)}}{\alpha}) \end{array} \right.$$

Under a risk neutral measure, the analytical formula and the Monte Carlo simulation provide same bond yields results. The model parameters determine the yield curve shape. For the drift term parameters, the mean reversion speed parameters  $\alpha$  and  $\beta$  increase the curvature of the yield and drives a higher Bond Yield. Increasing mean reversion level  $\phi$  can reduce the steepness of the bond yield curve. Bond investor benefit from both short-term and long-term volatility, so increasing in  $\sigma$  or  $\eta$  can increase the bond price and reduce bond yield. However, the interest rate path would be more volatile and introduce more interest rate risks which the investors should consider hedging.

Using a T1 maturity bond as a numeraire, the analytical expression of the certain bond option we studies is

$$v_t = P_t(T_2)\Phi(d_+) - P_t(T_1)K\Phi(d_-)$$

where

$$d_{\pm} = \frac{1}{\Omega} \log\left(\frac{P_t(T_2)}{KP_t(T_1)}\right) \pm \frac{1}{2}\Omega$$

$$\Omega^2 = \sigma^2 \int_t^{T_1} (B_s(T_1) - B_s(T_2))^2 ds + \eta^2 \int_t^{T_1} (C_s(T_1) - C_s(T_2))^2 ds$$

In terms of the bond option pricing process, different pricing measure with corresponding numeraire has no impact on the option's process. The bond options' prices are same under risk-neutral and forward-neutral measure. Moreover, the black implied volatility shows a shape of a skew, sometimes smile. As we reduce the time to exercise (T1), the "smile" shape become more obvious. The IV curves' shape difference could be due to the varying interest rate simulations. Sometimes the generated swap rate is relatively higher that the swaption have higher possibility to exercise. The swaption is less likely to exercise when interest rate is low. For both cases the curve is more weighted on the left side, which indicates that an ITM swaption is considered to be more valuable than the OTM ones for the special case we studied. Fund managers can quote different interest rate products by making reasonable modeling assumptions, hedging potential risks, or obtaining risk premium through exposure to interest rate fluctuations.